ACS APPLIED MATERIALS & INTERFACES

www.acsami.org

Research Article

Capacitively Coupled Plasma from Laser-Induced Graphene Points to Ozone as the Major Mediator of Antibacterial Activity

James O. Larkin, Sarah C. Mozden, Yieu Chyan, Qingxin Zheng, Paul Cherukuri,* James M. Tour, and Zachary T. Ball*

Cite This: *ACS Appl. Mater. Interfaces* 2023, 15, 45601−45605

Read Online

ACCESS | Metrics & More | Article Recommendations | Supporting Information

ABSTRACT: Low-temperature plasma is an emerging approach for the treatment of bacterial infections. Nonchemical treatments such as cold plasma offer potential solutions to antibiotic resistance. We investigated the use of laser-induced graphene as an inexpensive, lightweight, and portable electrode for generating cold plasma. At the same time, the mechanism or molecular mediators of cold plasma-induced antibacterial activity remain poorly understood. This study validates graphene as an efficient structure for producing therapeutic cold plasma, and this study also indicates that ozone is the primary mediator of antibacterial activity in graphene-mediated cold plasmas for bacterial growth under the conditions studied.

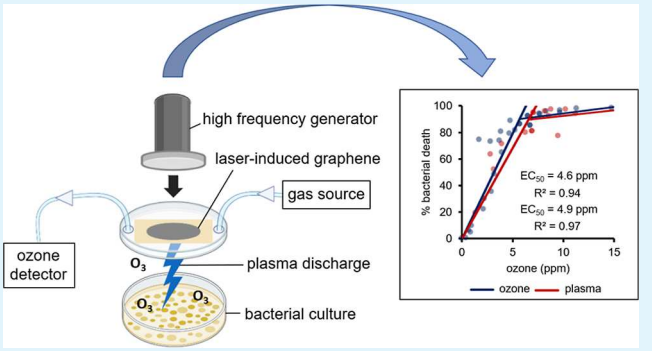

KEYWORDS: *graphene, cold plasma, antibacterial, ozone, reactive oxygen species, polyimide*

INTRODUCTION

Cold plasma (CP) technology is a promising alternative antibacterial agent with the potential to overcome resistance mechanisms that plague traditional antibiotic drugs.[1,2] This technology utilizes plasma, a partially ionized gas composed of electrons, ions, and reactive species, to eliminate microorganisms and inactivate viruses on surfaces, including wounds and other porous materials.[3−7] One of the main advantages of cold plasma for wound sanitization is its safety profile. Cold plasma does not generate heat, and several studies[8−10] indicate that therapy is safe for mammalian tissue and indeed is "without any known significant negative effects on healthy tissues."[11] CP also does not leave toxic residue on the wound surface,[7] can prevent biofilm formation,[12] and promotes wound healing by stimulating cell proliferation[5,13] and collagen synthesis.[14,15] Atmospheric plasma has also been employed to activate polymeric biomaterials for wound healing and antimicrobial delivery.[16,17] Additionally, cold-atmospheric plasma devices have been utilized for induction of immunogenic cell death of cancer cells in surgical cavities,[18] blocking cancer survival pathways,[19] and treating a variety of cancer cell lines.[20−24]

These investigations have also led to inquiries into the molecular mechanism of action of plasma therapeutics. Despite a robust history of investigation, the mechanism and exact nature of molecular mediators of cold plasma antibacterial activity are not known and remain the subject of current investigation.[1] It may be that the short lifetime[25] and complex composition of plasma discharge contribute to the analytical challenges associated with determining the impact of individual molecular species. A variety of reactive species have been postulated as playing a key role in observed effects, including peroxide, free radicals, and reactive nitrogen species.[26,27] For example, a recent report investigated hydrogen peroxide as one potential active agent in plasma-based antibacterial therapy but found that hydrogen peroxide was insufficient to account for the observed results.[1] Furthermore, cell death upon exposure to ozone from plasma is a complex biochemical phenomenon that has been extensively studied.[28−30]

CP for therapeutic applications has been generated in a variety of ways, including plasma jets and needles[1,31] as well as dielectric barrier discharge.[4,32] Access to inexpensive, robust, lightweight, and easily available components for plasma generation could enable plasma therapy in remote areas, low-resource settings, or as a compact portable treatment device. In this study, we report the efficacy of a capacitively coupled laser-induced graphene (LIG)-based plasma device for surface sanitization. By analyzing the ozone produced by the plasma discharge in a flow-through setup and comparing cell-killing results to those of a traditional external ozone generator, we

Received: June 26, 2023
Accepted: September 5, 2023
Published: September 19, 2023

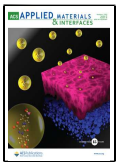

determined that the ozone produced within the plasma discharge is sufficient to explain the observed cell killing.

RESULTS

LIG is easily synthesized by laser irradiation of a wide variety of common polymer films, such as polyimide (e.g., Kapton, see Figure 1)[33−35] on a wide range of substrates.[36] The resulting

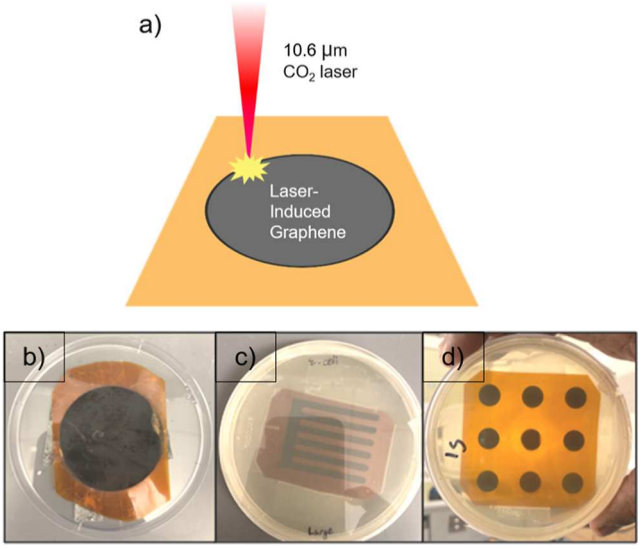

Figure 1. (a) Schematic of LIG synthesis on a polyimide film surface to form various patterns, including LIG deposits. (b−d) Petri dishes are 100 mm in diameter.

LIG exhibits high electrical conductivity, good flexibility, and low weight, making it an ideal material for use as an electrode in the generation of plasma.[33,34,37] A flexible electrode material could prove essential for localizing CP near real-world wounds that have unpredictable shapes that do not conform to the flat topologies of laboratory bacterial growth plates. Capacitively coupling an LIG material with an externally received field makes it possible to generate plasma cheaply and easily without the need for electrical connections.

The LIG for this study is easily synthesized through laser irradiation of a polyimide surface based on protocols previously reported (Figure 1a).[34] The ability to synthesize and pattern LIG into any desired dimensional shape and layout allows easy customization of the pattern to fit various applications. This method afforded a variety of graphene deposit rounded shapes to minimize arc discharge from graphene-Kapton edges (Figure 1b−d). The resulting LIG-layered materials exhibit good flexibility and low weight, making them an ideal electrode for the generation of plasma. We briefly examined a variety of LIG geometries (Figure 1b−d) but saw similar plasma-derived antibacterial performance, and all data reported here utilize the circular LIG pattern in Figure 1b.

To generate plasma through capacitive coupling with LIG, we make use of a commercially available high frequency, high voltage, and hand-held Tesla coil (Electro-Technic Products, Ltd.) that is capacitively coupled to an LIG material placed on the inner aspect of the lid on a closed Petri dish (Figure 2a). The LIG functions both as an electric field receiver and a dielectric barrier discharge material that generates plasma

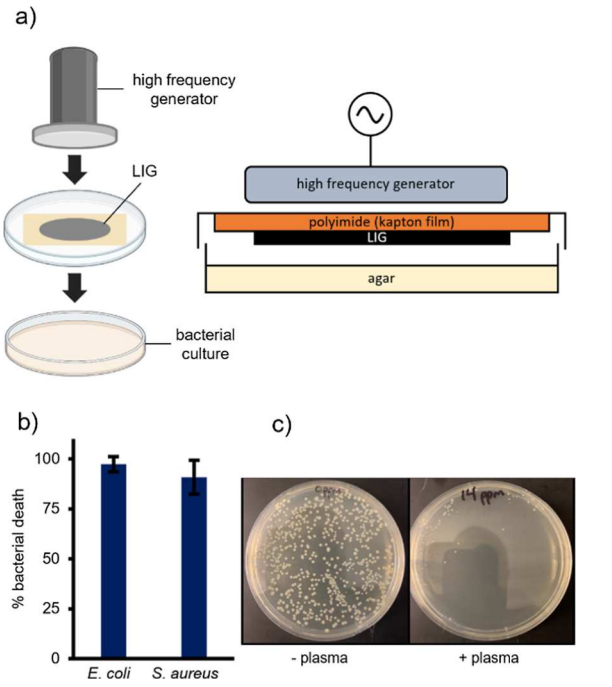

Figure 2. (a) Schematic illustrations of the high frequency generator applied to LIG in a bacterial culture. (b) *E. coli* and *S. aureus* % cell death after 2 min plasma exposure. (c) *E. coli* cell cultures with 0 and 14 ppm plasma ozone exposure over 5 min.

inside the Petri dish without the need to make physical electrode connections into the bacterial growth chamber.

The LIG affixed to the polyimide, upon which it was prepared, was mounted to the inside of a Petri dish lid (Figure 2a) with tape. After closing the lid on a bacterial culture, plasma antibacterial studies could then be conducted without opening or disturbing the bacterial colonies. Turning on the high frequency generator above the lid resulted in an immediately observable corona discharge from the LIG within the Petri dish (see Supporting Information).

We explored the antibacterial properties of this capacitively coupled plasma system against 2 different bacteria: *Escherichia coli* (Gram-negative) and *Staphylococcus aureus* (Gram-positive). After 2 min of exposure, significant bacterial death was observed, with >97% cell death observed for *E. coli* and >90% cell death observed for *S. aureus* (Figure 2b,c).

Having established that capacitively coupled plasma could induce bacterial cell death, we became interested in exploring the molecular mechanism of action responsible for the observed activity. Based on previous reports that ROS may be significant contributors, we first examined the response of an ROS indicator, Congo red, to plasma (Figure 3). Congo red is an azo dye sensitive to oxidants,[38] and bleaching has been used as a method to quantify ROS species generally.[39] When exposing both *E. coli* and Congo red to plasma, there was a positive correlation between the voltage input of the plasma generator (Supporting Information) and both increased bacterial killing and a change in absorbance of dye due to oxidative bleaching by ROS (Figure 3b,c).

Our Congo red studies pointed to ROS species as a significant mediator of cell death, and we hypothesized that one ROS in particular, ozone, may play a role in the observed antibacterial activity. We next sought to examine the relationship between plasma, ozone, specifically, and bacterial

https://doi.org/10.1021/acsami.3c09216
ACS Appl. Mater. Interfaces 2023, 15, 45601−45605

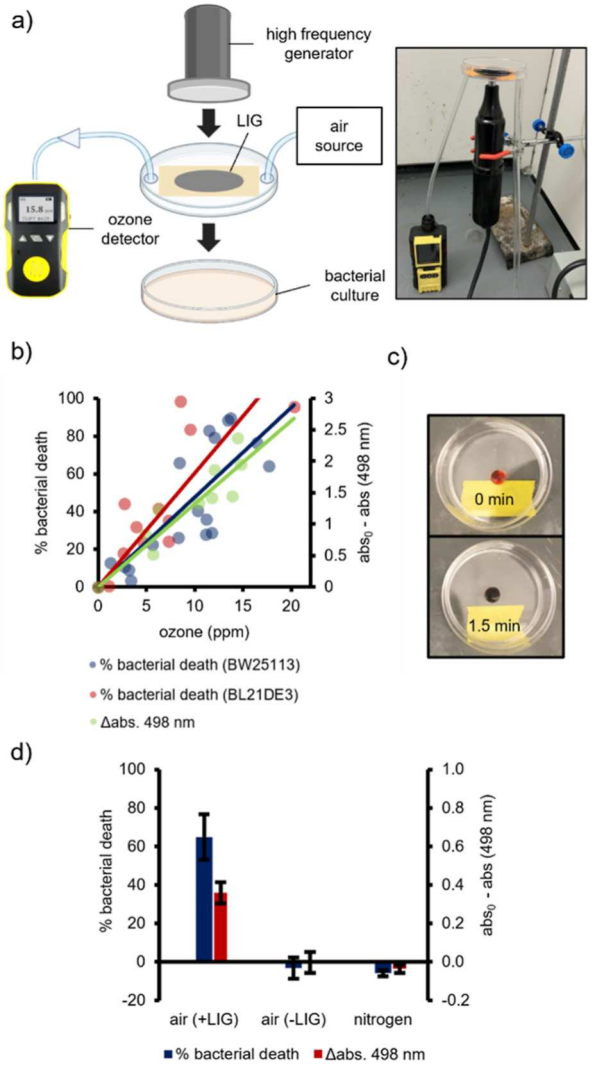

Figure 3. (a) Illustration and picture of the system for controlled ozone bacterial exposure to LIG-generated CP. (b) Absorbance of Congo red dye [100 mg/L, 100 μL, analytical standard Congo red (≥97.0%)] and *E. coli* % bacterial death as a function of ozone concentration over 2 min exposure. (c) Congo red (1 g/L, 10 μL, dye content ≥ 35%) color change after 1.5 min exposure to ozone generator. (d) Comparison of bacterial death and Congo red absorbance change between air with and without LIG and nitrogen gas systems for 2 min plasma exposure with air flowing at 35 psi.

cell death in a more quantitative way. In order to measure ozone levels in situ during plasma treatment, we measured ozone concentration by means of a flow-through design (Figure 3a). Measuring in situ ozone levels during plasma treatment allowed us to discover a positive correlation also exists between ozone levels and Congo red oxidative bleaching (Figure 3b, green data) and bacterial killing against two different cell lines (red, blue data). In addition, control experiments conducted under an inert atmosphere (N_2) and without LIG showed negligible bacterial cell killing (Figure 3d), lending further credence to the significant role of ozone in plasma therapy.

To more directly and quantitatively assess the extent to which ozone is responsible for the observed cell-killing behavior, we used the same flow-through setup (Figure 3a) to measure both the ozone concentration and cell killing observed for (i) plasma-based therapy (Figure 4a,b, red data)

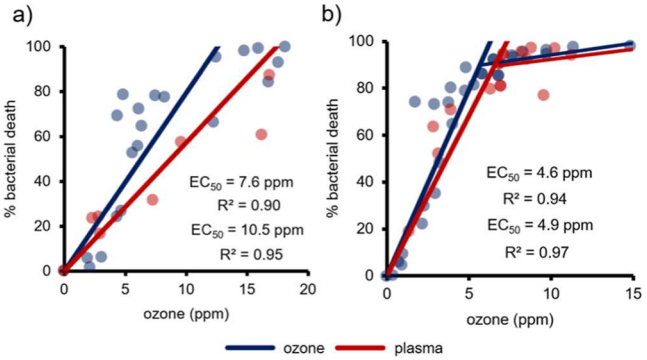

Figure 4. Bacterial cell death curves from the controlled ozone exposure system were generated with (a) BW25113 and (b) BL21DE3 strains of *E. coli* after 5 min of exposure.

and (ii) ozone alone, produced by a commercially available external ozone generator fed into the incoming air flow (blue data). In both instances, the ozone concentration could be conveniently controlled by regulating the air flow rate into the system (Figure 3a). Bacterial cell death curves were developed for two different strains of *E. coli* for plasma and ozone generator exposure (Figure 4a,b). The extent of bacterial cell death in plasma and external ozone generator experiments was statistically indistinguishable for both the BW25113 and BL21DE3 strains. The data suggest that ozone concentration is necessary and sufficient to explain the cell killing observed with the LIG-based capacitively coupled plasma generator. This finding is surprising given the complexity and diversity of reactive and/or high-energy species present in plasma, but may reflect the short diffusional lifetime and thus quite limited effect on cells of many such species in the plasma phase.

A novel system of CP therapy has been developed by using LIG as a flexible and cost-effective electrode for generating CP for surface or wound sanitization. The use of a polymer film for capacitively coupled plasma generation provides opportunities for using plasma easily and effectively in enclosed environments, in low-resource settings, and/or in situations demanding flexibility/mobility. Our findings also emphasize the significance of ozone as the primary reactive species responsible for bacterial cell death and indicate that plasma may be an effective approach for localized generation of ozone for bactericidal purposes.

■ ASSOCIATED CONTENT

Supporting Information

The Supporting Information is available free of charge at https://pubs.acs.org/doi/10.1021/acsami.3c09216.

Experimental details of LIG synthesis and methods for handling *E. coli* cell cultures, as well as additional Congo red absorbance and bacterial colony data (PDF) and video of plasma discharge from LIG surface (MP4)

■ AUTHOR INFORMATION

Corresponding Authors

Paul Cherukuri − *Institute of Biosciences and Bioengineering, Department of Electrical and Computer Engineering, and Rice Nexus, Rice University, Houston, Texas 77005, United States*; Email: cheru@rice.edu

https://doi.org/10.1021/acsami.3c09216
ACS Appl. Mater. Interfaces 2023, 15, 45601−45605

Zachary T. Ball − *Department of Chemistry and Institute of Biosciences and Bioengineering, Rice University, Houston, Texas 77005, United States;* orcid.org/0000-0002-8681-0789; Email: zb1@rice.edu

Authors

James O. Larkin − *Department of Chemistry, Rice University, Houston, Texas 77005, United States*

Sarah C. Mozden − *Department of Chemistry, Rice University, Houston, Texas 77005, United States*

Yieu Chyan − *Department of Chemistry, Rice University, Houston, Texas 77005, United States*

Qingxin Zheng − *Department of Chemistry, Rice University, Houston, Texas 77005, United States*

James M. Tour − *Department of Chemistry, Department of Computer Science, Smalley-Curl Institute and the NanoCarbon Center, and Department of Materials Science and NanoEngineering, Rice University, Houston, Texas 77005, United States;* orcid.org/0000-0002-8479-9328

Complete contact information is available at: https://pubs.acs.org/10.1021/acsami.3c09216

Notes

The authors declare no competing financial interest.

■ ACKNOWLEDGMENTS

We acknowledge support from the Robert A. Welch Foundation Research Grant C-1680 (Z.T.B.) and from DoD under DOD ONR N00014-19-1-2401. We acknowledge helpful conversations and experimental support from George Bennett, Yousif Shamoo, Erykah Pedro, Michael Swierczynski, and Matthew Peña. The BW25113 cell line was kindly provided by Yousif Shamoo.

■ REFERENCES

(1) Nicol, M. J.; Brubaker, T. R.; Honish, B. J.; Simmons, A. N.; Kazemi, A.; Geissel, M. A.; Whalen, C. T.; Siedlecki, C. A.; Bilén, S. G.; Knecht, S. D.; Kirimanjeswara, G. S. Antibacterial effects of low-temperature plasma generated by atmospheric-pressure plasma jet are mediated by reactive oxygen species. *Sci. Rep.* **2020**, *10*, 3066.

(2) Heinlin, J.; Isbary, G.; Stolz, W.; Morfill, G.; Landthaler, M.; Shimizu, T.; Steffes, B.; Nosenko, T.; Zimmermann, J.; Karrer, S. Plasma applications in medicine with a special focus on dermatology. *J. Dtsch. Dermatol. Ges.* **2011**, *8*, 968−976.

(3) Misra, N. N.; Jo, C. Applications of cold plasma technology for microbiological safety in meat industry. *Trends Food Sci. Technol.* **2017**, *64*, 74−86.

(4) Hoffmann, C.; Berganza, C.; Zhang, J. Cold Atmospheric Plasma: methods of production and application in dentistry and oncology. *Med. Gas Res.* **2013**, *3*, 21.

(5) Mohd Nasir, N.; Lee, B. K.; Yap, S. S.; Thong, K. L.; Yap, S. L. Cold plasma inactivation of chronic wound bacteria. *Arch. Biochem. Biophys.* **2016**, *605*, 76−85.

(6) Mirpour, S.; Fathollah, S.; Mansouri, P.; Larijani, B.; Ghoranneviss, M.; Mohajeri Tehrani, M.; Amini, M. R. Cold atmospheric plasma as an effective method to treat diabetic foot ulcers: A randomized clinical trial. *Sci. Rep.* **2020**, *10*, 10440.

(7) Filipić, A.; Gutierrez-Aguirre, I.; Primc, G.; Mozetič, M.; Dobnik, D. Cold Plasma, a New Hope in the Field of Virus Inactivation. *Trends Biotechnol.* **2020**, *38*, 1278−1291.

(8) Hüfner, A.; Steffen, H.; Holtfreter, B.; Schlüter, R.; Duske, K.; Matthes, R.; von Woedtke, T.; Weltmann, K.-D.; Kocher, T.; Jablonowski, L. Effects of Non-Thermal Atmospheric Pressure Plasma and Sodium Hypochlorite Solution on Enterococcus faecalis Biofilm: An Investigation in Extracted Teeth. *Plasma Processes Polym.* **2017**, *14*, 1600064.

(9) Baz, A.; Bakri, A.; Butcher, M.; Short, B.; Ghimire, B.; Gaur, N.; Jenkins, T.; Short, R. D.; Riggio, M.; Williams, C.; Ramage, G.; Brown, J. L. Staphylococcus aureus strains exhibit heterogenous tolerance to direct cold atmospheric plasma therapy. *Biofilm* **2023**, *5*, 100123.

(10) Kalghatgi, S.; Kelly, C. M.; Cerchar, E.; Torabi, B.; Alekseev, O.; Fridman, A.; Friedman, G.; Azizkhan-Clifford, J. Effects of Non-Thermal Plasma on Mammalian Cells. *PLoS One* **2011**, *6*, No. e16270.

(11) Braný, D.; Dvorská, D.; Halašová, E.; Škovierová, H. Cold Atmospheric Plasma: A Powerful Tool for Modern Medicine. *Int. J. Mol. Sci.* **2020**, *21*, 2932.

(12) Hage, M.; Khelissa, S.; Akoum, H.; Chihib, N.-E.; Jama, C. Cold plasma surface treatments to prevent biofilm formation in food industries and medical sectors. *Appl. Microbiol. Biotechnol.* **2022**, *106*, 81−100.

(13) Mongkolpobsin, K.; Sillapachaiyaporn, C.; Lertpatipanpong, P.; Boonruang, K.; Hwang, C.-Y.; Tencomnao, T.; Baek, S. J. Cold atmospheric microwave plasma (CAMP) stimulates dermal papilla cell proliferation by inducing β-catenin signaling. *Sci. Rep.* **2023**, *13*, 3089.

(14) Chatraie, M.; Torkaman, G.; Khani, M.; Salehi, H.; Shokri, B. In vivo study of non-invasive effects of non-thermal plasma in pressure ulcer treatment. *Sci. Rep.* **2018**, *8*, 5621.

(15) Fathollah, S.; Mirpour, S.; Mansouri, P.; Dehpour, A. R.; Ghoranneviss, M.; Rahimi, N.; Safaie Naraghi, Z.; Chalangari, R.; Chalangari, K. M. Investigation on the effects of the atmospheric pressure plasma on wound healing in diabetic rats. *Sci. Rep.* **2016**, *6*, 19144.

(16) Jhong, J.-F.; Venault, A.; Hou, C.-C.; Chen, S.-H.; Wei, T.-C.; Zheng, J.; Huang, J.; Chang, Y. Surface Zwitterionization of Expanded Poly(tetrafluoroethylene) Membranes via Atmospheric Plasma-Induced Polymerization for Enhanced Skin Wound Healing. *ACS Appl. Mater. Interfaces* **2013**, *5*, 6732−6742.

(17) Gaur, N.; Patenall, B. L.; Ghimire, B.; Thet, N. T.; Gardiner, J. E.; Le Doare, K. E.; Ramage, G.; Short, B.; Heylen, R. A.; Williams, C.; Short, R. D.; Jenkins, T. A. Cold Atmospheric Plasma-Activated Composite Hydrogel for an Enhanced and On-Demand Delivery of Antimicrobials. *ACS Appl. Mater. Interfaces* **2023**, *15*, 19989−19996.

(18) Chen, G.; Chen, Z.; Wang, Z.; Obenchain, R.; Wen, D.; Li, H.; Wirz, R. E.; Gu, Z. Portable air-fed cold atmospheric plasma device for postsurgical cancer treatment. *Sci. Adv.* **2021**, *7*, No. eabg5686.

(19) Guo, B.; Pomicter, A. D.; Li, F.; Bhatt, S.; Chen, C.; Li, W.; Qi, M.; Huang, C.; Deininger, M. W.; Kong, M. G.; Chen, H.-L. Trident cold atmospheric plasma blocks three cancer survival pathways to overcome therapy resistance. *Proc. Natl. Acad. Sci. U.S.A.* **2021**, *118*, No. e2107220118.

(20) Yan, D.; Wang, Q.; Adhikari, M.; Malyavko, A.; Lin, L.; Zolotukhin, D. B.; Yao, X.; Kirschner, M.; Sherman, J. H.; Keidar, M. A Physically Triggered Cell Death via Transbarrier Cold Atmospheric Plasma Cancer Treatment. *ACS Appl. Mater. Interfaces* **2020**, *12*, 34548−34563.

(21) Yao, X.; Yan, D.; Lin, L.; Sherman, J. H.; Peters, K. B.; Keir, S. T.; Keidar, M. Cold Plasma Discharge Tube Enhances Antitumoral Efficacy of Temozolomide. *ACS Appl. Bio Mater.* **2022**, *5*, 1610−1623.

(22) Yu, H.; Wang, Y.; Wang, S.; Li, X.; Li, W.; Ding, D.; Gong, X.; Keidar, M.; Zhang, W. Paclitaxel-Loaded Core−Shell Magnetic Nanoparticles and Cold Atmospheric Plasma Inhibit Non-Small Cell Lung Cancer Growth. *ACS Appl. Mater. Interfaces* **2018**, *10*, 43462−43471.

(23) Gjika, E.; Pal-Ghosh, S.; Tang, A.; Kirschner, M.; Tadvalkar, G.; Canady, J.; Stepp, M. A.; Keidar, M. Adaptation of Operational Parameters of Cold Atmospheric Plasma for in Vitro Treatment of Cancer Cells. *ACS Appl. Mater. Interfaces* **2018**, *10*, 9269−9279.

(24) Gjika, E.; Pal-Ghosh, S.; Kirschner, M. E.; Lin, L.; Sherman, J. H.; Stepp, M. A.; Keidar, M. Combination therapy of cold

atmospheric plasma (CAP) with Temozolomide in the treatment of U87MG glioblastoma cells. *Sci. Rep.* **2020**, *10*, 16495.
(25) Umapathi, R.; Reddy, P. M.; Rani, A.; Venkatesu, P. Influence of additives on thermoresponsive polymers in aqueous media: a case study of poly(N-isopropylacrylamide). *Phys. Chem. Chem. Phys.* **2018**, *20*, 9717−9744.
(26) Laroussi, M.; Leipold, F. Evaluation of the roles of reactive species, heat, and UV radiation in the inactivation of bacterial cells by air plasmas at atmospheric pressure. *Int. J. Mass Spectrom.* **2004**, *233*, 81−86.
(27) Bekeschus, S.; Kolata, J.; Winterbourn, C.; Kramer, A.; Turner, R.; Weltmann, K. D.; Bröker, B.; Masur, K. Hydrogen peroxide: A central player in physical plasma-induced oxidative stress in human blood cells. *Free Radical Res.* **2014**, *48*, 542−549.
(28) Girgin Ersoy, Z.; Barisci, S.; Dinc, O. Mechanisms of the Escherichia coli and Enterococcus faecalis inactivation by ozone. *LWT* **2019**, *100*, 306−313.
(29) Kadono, T.; Tran, D.; Errakhi, R.; Hiramatsu, T.; Meimoun, P.; Briand, J.; Iwaya-Inoue, M.; Kawano, T.; Bouteau, F. Increased Anion Channel Activity Is an Unavoidable Event in Ozone-Induced Programmed Cell Death. *PLoS One* **2010**, *5*, No. e13373.
(30) Lunov, O.; Zablotskii, V.; Churpita, O.; Chánová, E.; Syková, E.; Dejneka, A.; Kubinová, Š. Cell death induced by ozone and various non-thermal plasmas: therapeutic perspectives and limitations. *Sci. Rep.* **2014**, *4*, 7129.
(31) Pei, X.; Lu, X.; Liu, J.; Liu, D.; Yang, Y.; Ostrikov, K.; Chu, P. K.; Pan, Y. Inactivation of a 25.5 μm Enterococcus faecalis biofilm by a room-temperature, battery-operated, handheld air plasma jet. *J. Phys. D: Appl. Phys.* **2012**, *45*, 165205.
(32) Weltmann, K.-D.; Polak, M.; Masur, K.; von Woedtke, T.; Winter, J.; Reuter, S. Plasma Processes and Plasma Sources in Medicine. *Contrib. Plasma Phys.* **2012**, *52*, 644−654.
(33) Ye, R.; James, D. K.; Tour, J. M. Laser-Induced Graphene. *Acc. Chem. Res.* **2018**, *51*, 1609−1620.
(34) Li, J. T.; Stanford, M. G.; Chen, W.; Presutti, S. E.; Tour, J. M. Laminated Laser-Induced Graphene Composites. *ACS Nano* **2020**, *14*, 7911−7919.
(35) Lin, J.; Peng, Z.; Liu, Y.; Ruiz-Zepeda, F.; Ye, R.; Samuel, E. L. G.; Yacaman, M. J.; Yakobson, B. I.; Tour, J. M. Laser-induced porous graphene films from commercial polymers. *Nat. Commun.* **2014**, *5*, 5714.
(36) Chyan, Y.; Ye, R.; Li, Y.; Singh, S. P.; Arnusch, C. J.; Tour, J. M. Laser-Induced Graphene by Multiple Lasing: Toward Electronics on Cloth, Paper, and Food. *ACS Nano* **2018**, *12*, 2176−2183.
(37) Xie, J.; Chen, Q.; Suresh, P.; Roy, S.; White, J. F.; Mazzeo, A. D. Paper-based plasma sanitizers. *Proc. Natl. Acad. Sci. U.S.A.* **2017**, *114*, 5119−5124.
(38) Kondru, A. K.; Kumar, P.; Chand, S. Catalytic wet peroxide oxidation of azo dye (Congo red) using modified Y zeolite as catalyst. *J. Hazard. Mater.* **2009**, *166*, 342−347.
(39) Wang, J.; Guo, Y.; Liu, B.; Jin, X.; Liu, L.; Xu, R.; Kong, Y.; Wang, B. Detection and analysis of reactive oxygen species (ROS) generated by nano-sized TiO2 powder under ultrasonic irradiation and application in sonocatalytic degradation of organic dyes. *Ultrason. Sonochem.* **2011**, *18*, 177−183.

https://doi.org/10.1021/acsami.3c09216
ACS Appl. Mater. Interfaces 2023, 15, 45601−45605